

# Geophysical Research Letters

## RESEARCH LETTER

10.1029/2019GL086586

### Key Points:

- Mean value of ensemble spreads (ESP) for drought Indian summer monsoon rainfall (ISMR) years is larger than flood years in reforecasts
- Ensemble means ISMR composite anomalies during drought years shows better agreement with observed in comparison to flood years
- Smaller ESP in flood years may suggest that ensemble prediction of ISMR tends to be overconfident and underestimate forecast uncertainty

### Supporting Information:

- Figure S1
- Table S1

### Correspondence to:

R. P. Shukla,  
rshukla2@gmu.edu

### Citation:

Shukla, R. P., & Shin, C.-S. (2020). Distinguishing spread among ensemble members between drought and flood Indian summer monsoon years in the past 58 years (1958–2015) reforecasts. *Geophysical Research Letters*, 47, e2019GL086586. <https://doi.org/10.1029/2019GL086586>

Received 10 DEC 2019

Accepted 28 JAN 2020

Accepted article online 29 JAN 2020

## Distinguishing Spread Among Ensemble Members Between Drought and Flood Indian Summer Monsoon Years in the Past 58 Years (1958–2015) Reforecasts

Ravi P. Shukla<sup>1</sup>  and Chul-Su Shin<sup>1,2</sup> 

<sup>1</sup>Center for Ocean-Land-Atmosphere Studies, George Mason University, Fairfax, VA, USA, <sup>2</sup>Department of Atmospheric, Oceanic, and Earth Sciences, George Mason University, Fairfax, VA, USA

**Abstract** This study examines the different characteristics of ensemble spread (ESP) between drought and flood years of Indian summer monsoon (ISM) during June to September mean using the Climate Forecast System version 2 (CFSv2). We have analyzed a set of 20-member ensemble seasonal reforecasts for 1958–2015 using CFSv2 initialized in April. The ESP of ISM Rainfall (ISMR) is negatively (positively) correlated with ISMR (NINO3.4) index, indicating that ESP in drought ISMR years seems to be larger than that in flood years. The mean value of ESP for drought ISMR years is larger than flood years. The spatial structure of ISMR composite anomalies during drought years shows better agreement with observed rainfall anomalies in comparison to flood years. As a result, smaller ESP in flood years may suggest that ensemble prediction of ISMR in flood years tends to be overconfident and less reliable due to underestimate of forecast uncertainty, compared to drought years.

## 1. Introduction

The Indian summer monsoon (ISM) rainfall (ISMR) is often defined by June to September (JJAS) mean rainfall over Indian landmass, which represents around 60–90% of total annual rainfall over most of the Indian subcontinent (Joshi & Rajeevan, 2006). Therefore, unusual anomalous ISMR such as drought and flood can cause devastating damage in agricultural production and water resource management in India (Gadgil & Gadgil, 2006). A drought (flood) year of ISM results from many processes and phenomena over its surrounding ocean, atmosphere, and land. For example, the El Niño–Southern Oscillation (ENSO) is the largest and most important climate variation on seasonal-to-interannual time scales, and it has a major impact on the atmospheric circulation and precipitation over Asia primarily in summer (Rasmusson & Carpenter, 1983; Shukla & Paolin, 1983; Shin et al., 2019; Wang et al., 2000). Many studies have shown that ISMR tends to be modulated by ENSO, that is, ISMR becomes weaker (stronger) during developing El Niño (La Niña) years (Kirtman & Shukla, 2000; Lau & Nath, 2000; Webster & Yang, 1992), although this negative correlation between indices of ENSO and ISMR has been weaker during recent decades (Krishna Kumar et al., 1999).

Many previous studies have used fully coupled climate ensemble forecast system to evaluate seasonal prediction skill and predictability of ISMR in the context of a deterministic seasonal forecast (i.e., ensemble mean prediction) and/or a probabilistic seasonal forecast using ensemble spread (Abhilash et al., 2015; Bauer et al., 2015; Kulkarni et al., 2012; Palmer et al., 2005; Saha et al., 2019). In contrast, relatively little attention has been paid to year-to-year variation of ensemble spread (ESP) of ISMR prediction, which may indicate the forecast uncertainty of the deterministic forecast. In particular, due to lack of long record of seasonal ensemble reforecasts using a state-of-the-art coupled climate model (i.e., most of them start from 1979), the forecast uncertainty between drought and flood years of ISM in the forecast system has not been addressed, in combination with assessment of prediction skill of ensemble mean forecasts.

Recently, a set of seasonal ensemble reforecasts for 58 years (1958–2015) had been conducted at the Center for Ocean-Land-Atmosphere Studies using National Centers for Environmental Prediction (NCEP) Coupled Forecast System version 2 (CFSv2; Saha et al., 2014; Huang et al., 2017). The CFSv2 model has been widely used to examine the seasonal prediction and predictability of the ENSO, ISM, and other important processes of atmosphere and ocean in the reforecasts and long-term simulations (Huang et al., 2017; Kim et al., 2012; Shukla et al., 2017; Sahana & Ghosh, 2018; Shin et al., 2019; Shukla, Huang, Dirmeyer, Kinter, Shin, et al.,

2019, Shukla, Huang, Dirmeyer, & Kinter, 2019; Zhu et al., 2012; Zhu & Shukla, 2013). More importantly, Huang et al. (2017) demonstrated that the ENSO prediction skill in 1958–1978 is comparable to that for 1979–2014 for the onset and development of ENSO events, although the skill of the earlier predictions declines faster for the ENSO decay.

In this study, we have analyzed a set of 20-member ensemble CFSv2 seasonal reforecasts for 58 years (1958–2015) initialized in April. We attempt to see if any distinguishing feature of ESP between flood and drought ISM years exists. For this purpose, we have selected drought and flood ISM years respectively based on normalized ISMR index (ISMRI) over Indian landmass in the past 58-year reforecasts, as to be shortly explained. Our results demonstrate that the mean ESP is larger for the drought years than the flood years, indicating that the ensemble predictions in the flood years tend to underestimate forecast uncertainty. Also, predicted ISMR anomalies for the drought years are in better agreement with observed one, in comparison to flood years. We further demonstrate that when ESP in normal monsoon years is large, predicted ISMR anomalies depict better agreement with the observed one except for a few years. A possible cause for this exception we will explore in section 3. The remainder of this paper is organized as follows. Section 2 briefly describes the model, the experimental design, and verification data sets. Section 3 presents ESP during flood, drought, and normal years of ISMR in reforecasts and its relationship to prediction skill of ISMR anomalies. A summary and discussion are given in section 4.

## 2. Model Description, Experimental Design, and Observational Data Sets

The coupled general circulation model used in this study is NCEP CFSv2 (Saha et al., 2014), which includes atmospheric, oceanic, sea ice, and land components. In this study, a revised version of coupled CFSv2 was used with adjusted parameters for sea ice albedo to maintain realistic multiyear sea ice cover in the Arctic Ocean (Huang et al., 2015). The ocean initial conditions (ICs) were from five instantaneous restart files of the European Centre for Medium-Range Weather Forecasts Ocean Reanalysis System 4 (Balmaseda et al., 2013) for 1958–2015. The land, atmosphere, and sea ice ICs were assembled from several different data sources. Since 1979, atmosphere, land, and sea ice ICs were from the Climate Forecast System Reanalysis (Saha et al., 2010). For the period 1958–1978, on the other hand, the atmospheric ICs were interpolated from the ERA-40 reanalysis (Uppala et al., 2005), and the land ICs were taken from the reprocessed 3-hourly National Aeronautics and Space Administration Global Land Data Assimilation System, version 2.0 analysis on a  $1^\circ \times 1^\circ$  (Rodell et al., 2004; Rui & Beaudoing, 2015). An ensemble reforecast of 20 members is generated by matching each of the five ocean ICs at 00Z 1 April with the atmospheric and land ICs at 00Z of the first four days of April while the sea ice initial state is fixed at 00Z 1 April for all ensemble members. More details about April-initialized reforecasts is found in Huang et al. (2017). It is noteworthy that there is no systematic shift in predicted global rainfall and sea surface temperature (SST) resulting from inconsistent data sources of land, atmosphere, and sea ice ICs before and after 1979.

The India Meteorological Department (IMD) gridded rainfall data at  $0.25^\circ \times 0.25^\circ$  grid used for the period 1958–2015 (Pai et al., 2013). Monthly gridded Global Precipitation Climatology Project (GPCP v2.2; Adler et al., 2003) at a grid resolution of  $2.5^\circ \times 2.5^\circ$  longitude for the period 1979–2015 is used in this study. The observed SST used for verification is the global monthly Extended Reconstructed SST, version 4 (ERSSTv4; Huang et al., 2014; Liu et al., 2014) for 1958–2015 on a  $2^\circ \times 2^\circ$  grid. The monthly SST fields are from the National Oceanic and Atmospheric Administration optimum interpolation (OI) SST analysis, version 2 (OISST v2) on a  $1^\circ \times 1^\circ$  grid for the period of 1982–2015 (Reynolds & Smith, 1995). In this study, a drought (flood) year is defined as when the ISMRI anomaly is below (above)  $-1$  ( $+1$ ) standard deviation of standardized ISMR index and when greater than 40% of the Indian subcontinent is under a drought (flood) condition.

## 3. Results

We discuss the characteristic features of ISMR over Indian landmass in April-initialized CFSv2 reforecasts and explore its connection with rainfall over the Indo-Pacific domain (Figure 1). Whereas CFSv2 seems to capture the main GPCP precipitation pattern over India seen in Figure 1a, including enhanced rainfall over western Ghats of India, eastern and central India (not shown), the model quantitatively demonstrates a severe dry bias over northern India with precipitation deficit up to 4.5 mm/day and an excessive rainfall in the central Indian Ocean and in subtropical northern Pacific Ocean (Figure 1b). The cause for the

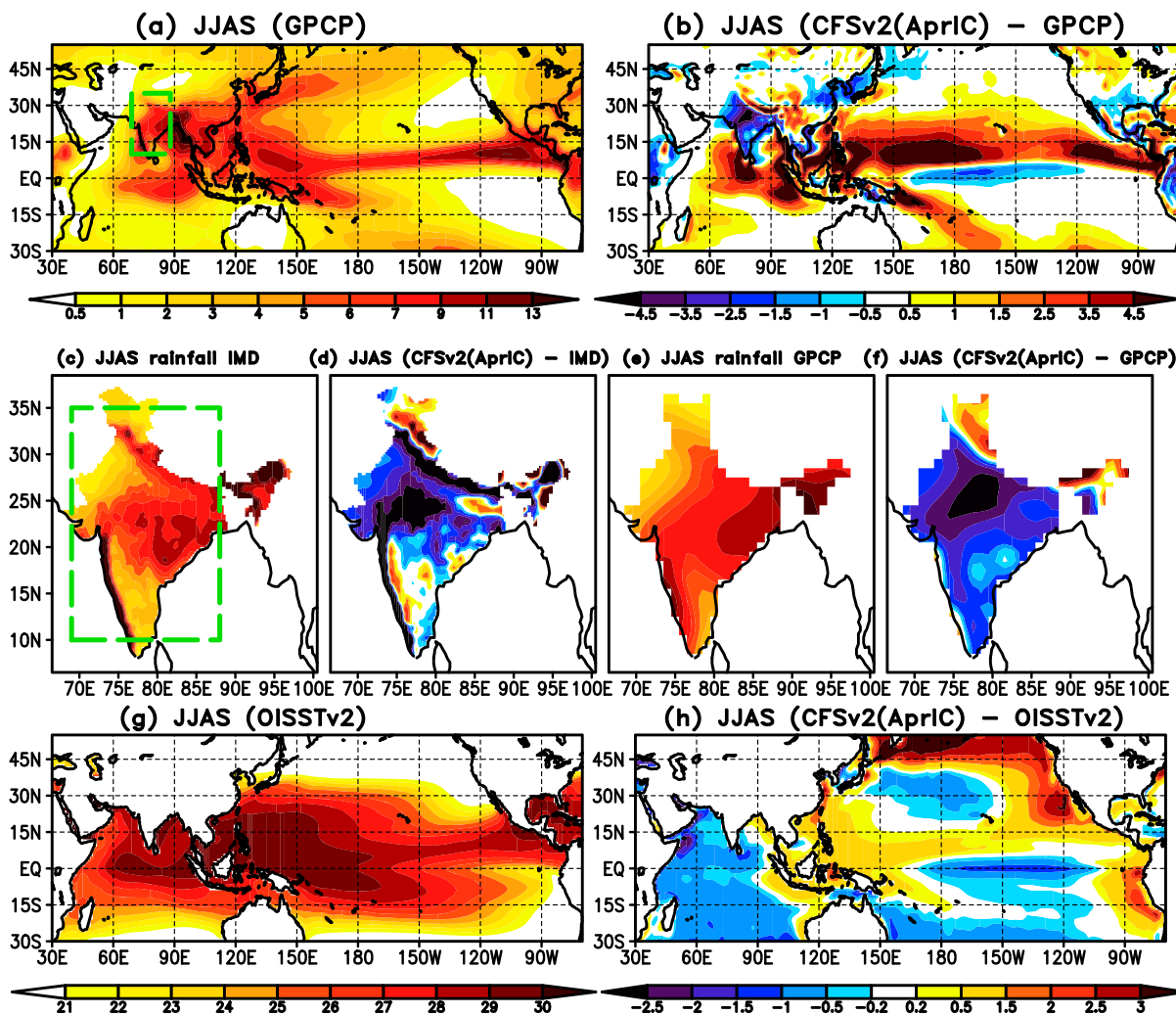


**Figure 1.** (a) The spatial distributions of JJAS mean climatology of GPCP rainfall over the tropical region for period 1979–2015 and (b) climatological biases relative to GPCP for April-initialized CFSv2 reforecasts. The scale for the magnitude for rainfall in mm/day is shown below these panels. (c) The JJAS mean climatology of IMD rainfall and (b) climatological biases relative to IMD rainfall for reforecasts. (e,f) As in (c,d) but for GPCP for period 1979–2015. (g) JJAS mean climatology of OISSTv2 for period 1982–2015 and (h) climatological bias relative to OISSTv2 for reforecasts. The scale for the magnitude for SST in °K is shown below these panels. Standard deviation of ensemble mean rainfall is approximately 10% to 30% of ensemble mean rainfall.

enhancement and northward shift of intertropical convergence zone near 10°N in CFSv2 model is discussed in Shukla and Huang (2015). The reforecasts depict a large dry bias over Indian landmass with respect to IMD rainfall, but magnitude of rainfall bias over southern eastern India is negligible (Figures 1c and 1d). It can be seen that major observed precipitation is over the oceanic warm pool region in the Indo-Pacific domain (Figure 1a) where SST lies between the 28 °C to 30 °C (Figure 1g). There may be several causes for underestimation of summer rainfall over Indian landmass in the reforecasts. It is found that model reforecasts depict a cold bias over the Arabian Sea (Figure 1h) and also produce excessive surface convergence over the equatorial Indian Ocean (not shown), which may reduce the moisture transport toward the Indian subcontinent region (Levine et al., 2013; Shukla & Huang, 2015).

Figure 2 shows year-to-year variation of ISMRI for ensemble mean and all members, ESP and NINO3.4 SST index for 1958–2015. The large blue squares represent anomalies of ensemble mean ISMRI over Indian landmass (green box in Figure 1c: 10–35°N, 69–88°E) in reforecasts. The standard procedure has been used to calculate anomaly. For example, for reforecasts initialized in April, the climatology for these reforecasts was removed. Anomalies of each ensemble member are computed from the climatology of ensemble mean (small blue squares in Figure 2). The correlation between ISMRI and JJAS mean NINO3.4 index (green

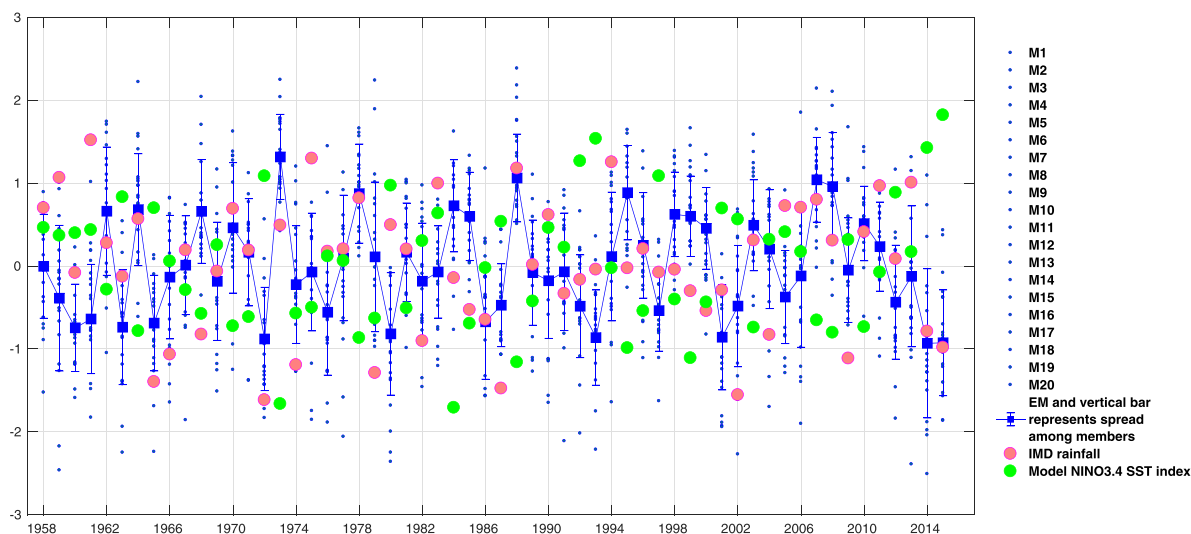


**Figure 2.** Year-to-year variation of season mean JJAS ISMR index (green box in Figure 1c: 10–35°N, 69–88°E) anomaly for ensemble mean of 20 members in large blue square in April-initialized reforecasts and vertical bar represents the spread among members. Each ensemble member is indicated by small blue circle. Green circle corresponds to JJAS NINO3.4 index anomaly in reforecasts. Pink circle corresponds to variation of JJAS IMD rainfall anomaly.

circle) for 1958–2015 is  $-0.87$  in the reforecasts whereas  $-0.51$  in observation using IMD rainfall (pink circle in Figure 2) and National Oceanic and Atmospheric Administration ERSSTv4 (not shown). This may suggest that in the reforecasts, India tends to experience depressed (enhanced) rainfall in summer when the tropical eastern Pacific SST is above (below) normal with overly strong negative correlation than the observation. The vertical bar in Figure 2 represents the ensemble spread among 20 members with respect to ensemble mean ISMRI anomaly each year. It can be seen that the range of vertical bar varies year to year, implying that the forecast uncertainty of ISMRI is not uniform in time in the April IC reforecasts. The temporal correlation between predicted and observed ISMRI is statistically significant over Indian rainfall index for periods 1979–2015 and 1997–2015 (Table S1 in the supporting information).

We have displayed a scatter plot between ESP of ISMRI and JJAS mean SST averaged over NINO3.4 region (hereafter NINO3.4 SST) during 1958–2015 (Figures 3a and S1). In general, it is found that there is one group of 13 years (red font) when ESP is low (mean ESP of those years =  $0.58$  mm/day) and range of NINO3.4 SST is between  $24.5^{\circ}\text{C}$  and  $26.0^{\circ}\text{C}$ . Ensemble mean of ISMRI ( $5.28$  mm/day) for these years is high in comparison to other years. On the other hand, there is another group of 11 years (blue font) when ESP is higher (mean ESP of those years =  $0.67$ ) and range of NINO3.4 SST is between  $27.0^{\circ}\text{C}$  and  $28.5^{\circ}\text{C}$ . The ensemble mean of ISMRI ( $3.66$  mm/day) is low in comparison to other years. To explore relationship between ESP of ISMRI and NINO3.4 SST nicely, we have divided the ESP for a given year by the ensemble mean rainfall for that year to obtain the normalized ESP. It is a well-known property of rainfall variability that high mean rainfall areas have high standard deviations generally (not shown), and by normalizing with the mean rainfall, the effect of SST anomalies on ESP is better estimated. Figure 3b displays scatter plot between normalized ESP of ISMRI and NINO3.4 SST. The scatter plot reveals nicely clustering of flood ISM years (red font; ESP =  $0.11$ ) when ESP is low and clustering of drought ISMR years (blue font; ESP =  $0.18$ ) when ESP is large. The normalized ESP of ISMRI is negatively correlated with the ensemble mean ISMRI (correlation coefficient =  $-0.74$ ; Figure 4a) and positively correlated with the summer NINO3.4 SST index (correlation coefficient =  $0.63$ ; Figure 4b), indicating that ESP in drought ISM years seems to be larger than that in flood years in reforecasts. To quantify the ensemble spread of ISMRI during flood and drought years, we have selected 13 strong ISM years (e.g., 1973 and 2008) and 11 weak ISM years (e.g., 1965 and 2014). It is found that mean ESP during flood years is  $0.58$  mm/day, which is lower than the mean ESP during drought ISM years ( $0.67$  mm/day) (Table S2). For case study, we have selected 9 flood (8 drought) years in which the ensemble mean JJAS mean NINO3.4 index is approximately less than  $-1$  (greater than  $+1$ ) standard deviation, referred to as La Niña and El Niño years. It is also confirmed that mean ESP of ISMRI over India is larger during El Niño years than La Niña years (Table S2).

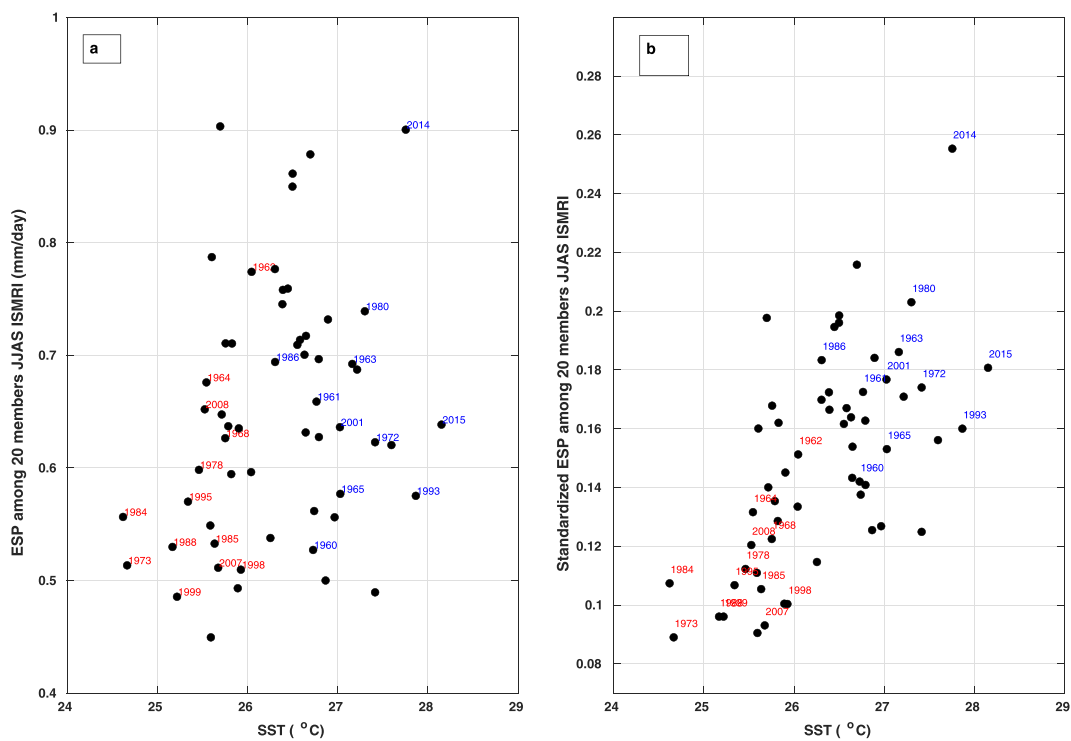


**Figure 3.** (a). Scatter plot between JJAS mean NINO3.4 index and ESP for JJAS ISMR index over India ( $10^{\circ}$ – $35^{\circ}$ N,  $69^{\circ}$ – $88^{\circ}$ E) in reforecasts for period 1958–2015.  
(b) As in (a) but for JJAS mean NINO3.4 index and standardized ESP for JJAS ISMR index.

It is necessary to mention that there is one group of 8 years (example, 1959, 1994) when normalized ESP is comparably larger (Figure 4a; black line). But according to our criteria, these years are normal monsoon years.

To explore the relationship between the ESP and prediction skill of ISMR anomalies, we have calculated area average of JJAS mean rainfall anomalies over Indian landmass in reforecasts and IMD rainfall (Figure S2)

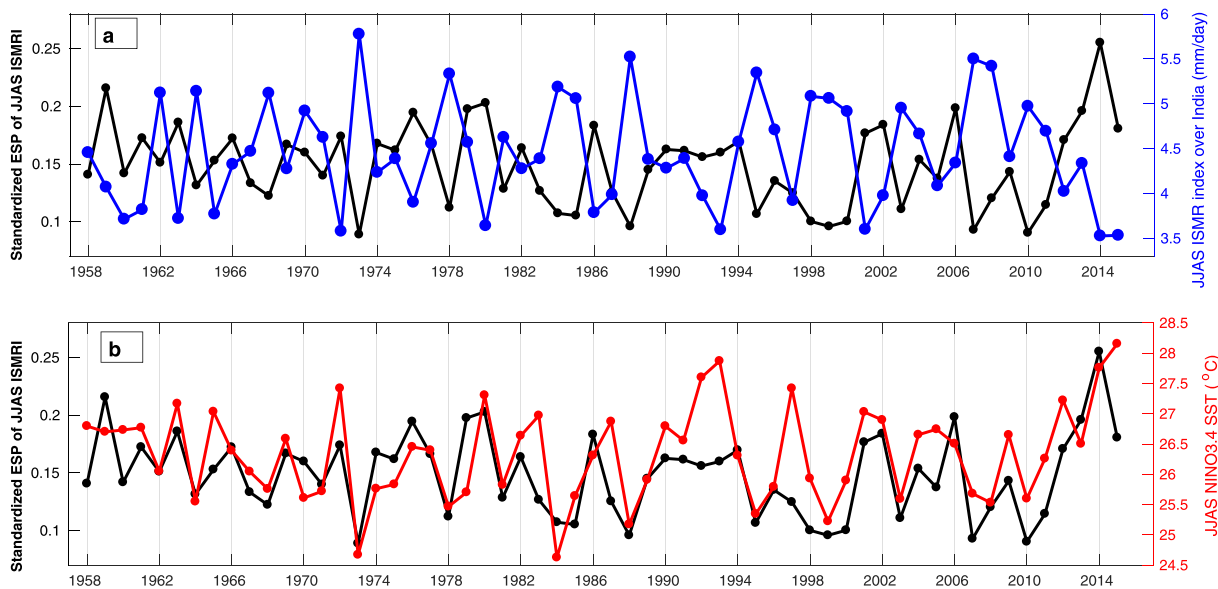


**Figure 4.** (a). Year-to-year variation of standardized ESP for JJAS ISMR index over Indian landmass ( $10^{\circ}$ – $35^{\circ}$ N,  $69^{\circ}$ – $88^{\circ}$ E) in black (scale in left side on Y axis) and JJAS ISMR index in blue (scale in right side on Y axis). (b) As in (a) but for standardized ESP for JJAS ISMR index and JJAS NINO3.4 index (red).

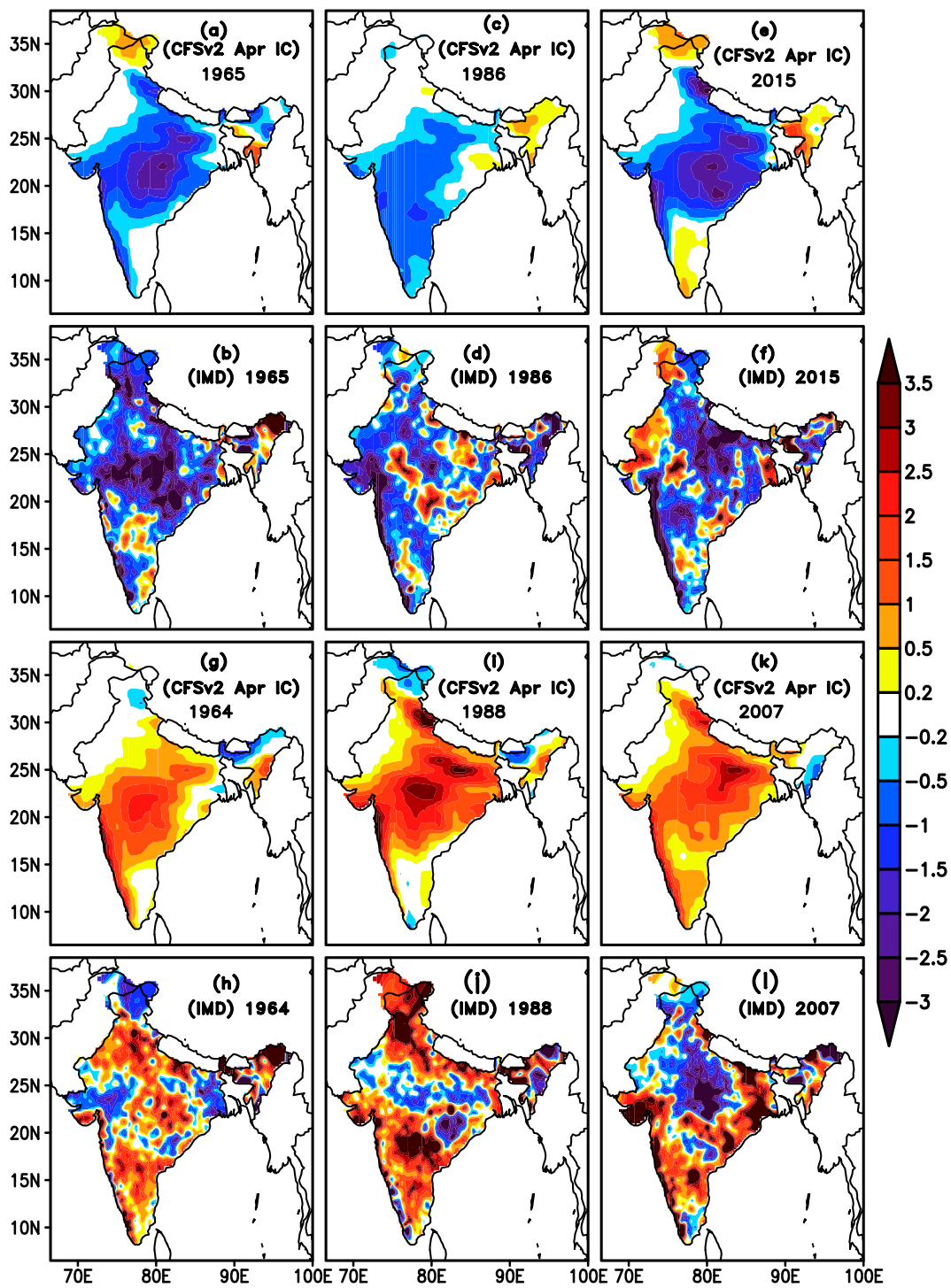


**Figure 5.** Spatial distribution of JJAS rainfall anomalies in 1965 (drought year in model) from (a) reforecasts and (b) IMD rainfall. (c, d) As in (a,b) but for year 1986. (e,f) As in (a,b) but for year 2015. The JJAS rainfall anomalies in 1964 (flood year in model) from (g) reforecasts and (h) IMD rainfall. (i,j) As in (g,h) but for year 1988. (k,l) As in (g,h) but for year 2007.

and spatial correlation between predicted and observed ISMR anomalies for period 1958–2015 (Figure S3). There are 9 (7) years out of 11 (13) drought (flood) ISM years in reforecasts in which ISMRI anomalies depict same sign of IMD ISMRI anomalies. It is notable that the sign of rainfall anomalies in 6 El Niño years out of

8 years in reforecast depict the same sign of IMD ISM anomalies where it is 5 La Niña years out of 9 years. The spatial pattern correlation value of ISMR anomalies between reforecast and observation is slightly higher during El Niño years than La Niña years (Table S3; Figure S2).

Figure 5 displays predicted and observed ISMR anomalies in three drought (flood) ISM years. For the drought ISM years, it is found that there is large negative rainfall anomaly over core monsoon region especially in 1965 (Figure 5a) and 2015 (Figure 5e) in reforecasts. Model reforecasts show better agreement with the IMD rainfall anomalies during 1965 (Figure 5b), 1986 (Figure 5d) and 2015 (Figure 5f). The spatial correlation between reforecasts and IMD rainfall anomalies for years 1965, 1986, and 2015 are 0.31, 0.11, and 0.27, respectively (Table S3). During flood ISM years, model reforecasts (Figures 5g, 5i, and 5k) depict positive rainfall anomalies over most of India landmass, and spatial structure of ISMR anomalies in these years in reforecasts does not show good agreement with IMD rainfall anomalies (Figures 5h, 5j, and 5l). The spatial correlation between reforecasts and IMD rainfall anomalies for years 1964, 1988, and 2007 are 0.06, -0.03, and 0.04. The spatial structure of composite ISMR anomalies over India during 8 El Niño years in reforecasts is in better agreement with observed ones in comparison to 9 La Niña years (Figure S4).

During normal monsoon years (e.g., 1966 and 1994), the model predicts the same sign of the ISMRI as the IMD rainfall does (Figure S1) and spatial correlation between reforecasts and IMD rainfall anomalies for these years are positive (Figure S2). We have also found that for 1959 and 2013, predicted ISMRI do not agree with observed one and their spatial correlations are also negative, but their ESPs are equivalent to that of drought years. It may raise the following question: For both years, why is the seasonal prediction skill bad, although the ESP is large? It is evident that only one or two members predict ISMRI anomaly far away from the ensemble mean value in both years, responsible for large ESP, which may cause this exception (Figure 2). For example, rainfall anomaly of each member from ensemble mean in 1959 is -2.09, -1.80, -0.89, -0.81, -0.46, -0.29, -0.17, -0.13, -0.03, 0.15, 0.21, 0.22, 0.29, 0.32, 0.43, 0.56, 0.82, 0.98, 1.29, and 1.38 mm/day, and the first two values are outliers that account for large ESP in 1959.

#### 4. Summary and Discussion

This study presents the different characteristics of ensemble spread between drought and flood years of ISM using 20-member ensemble seasonal reforecasts for 58 years (1958–2015). Consistent with previous studies (Shukla & Huang, 2015; Shukla et al., 2017; Sahana & Ghosh, 2018), we have also found that April-initialized CFSv2 reforecasts underestimate summer rainfall over Indian landmass.

The ensemble spread (ESP) of ISMRI is negatively (positively) correlated with ISMRI (NINO3.4 SST index). The scatter plot between normalized ESP of ISMRI and NINO3.4 SST index confirmed that the clustered drought years (flood years) are below (above) 26.0 °C (27.0 °C). The drought ISM years have larger ESP than the flood years. To quantify the ESP of ISMRI during flood and drought years, we have selected 13 flood and 11 drought ISM years in the reforecasts. The mean ESP over Indian landmass for the drought ISM years is larger than for the flood years. It is also found that the spatial structure of ensemble mean ISMR composite anomalies for the drought years are in better agreement with observed ones in comparison to those for the flood years. Our results also demonstrate that among normal monsoon years, if the ESP is comparable to that of drought years, predicted ISMRI in reforecasts tends to show a good agreement with the observed one. On the other hand, there are some exceptions; even though the ESP is large enough in a few normal ISM years, the model is not able to predict the sign of observed ISM anomalies with negative spatial correlation. It is found that an exceptionally large departure of only a couple of members from the ensemble mean may lead to large ESP in those years. Therefore, we argue that the spread among ensemble members within a certain range is one of the important factors for improving ISMR prediction skill not only in seasonal reforecasts with CFSv2 but probably also in other state-of-the-art coupled general circulation models.

#### References

- Abhilash, S., Sahai, A. K., Borah, N., Joseph, S., Chattopadhyay, R., Sharmila, S., et al. (2015). Improved spread-error relationship and probabilistic prediction from the CFS-based Grand Ensemble Prediction System. *Journal of Applied Meteorology and Climatology*, 54(7), 1569–1578. <https://doi.org/10.1175/JAMC-D-14-0200.1>
- Adler, R. F., Huffman, G. J., Chang, A., Ferraro, R., Xie, P. P., Janowiak, J., et al. (2003). The version-2 Global Precipitation Climatology Project (GPCP) monthly precipitation analysis (1979–present). *Journal of Hydrometeorology*, 4, 1147–1167.

#### Acknowledgments

Funding for this research work was provided by Grants from the National Science Foundation (1338427), the National Oceanic and Atmospheric Administration (NA14OAR4310160), and the National Aeronautics and Space Administration (NNX14AM19G). The computations were made on the Extreme Science and Engineering Discovery Environment (XSEDE) high-performance computing platform (Towns et al., 2014), and the computational resources are gratefully acknowledged. We would like to share our data to the scientific community that discussed in the manuscript through Zenodo (DOI: 10.5281/zenodo.3626206). The authors are grateful to two anonymous reviewers for their constructive comments and suggestions, which improved the quality of the manuscript significantly. The authors declare that they have no conflict of interest.

- Balmaseda, M. A., Mogensen, K., & Weaver, A. T. (2013). Evaluation of the ECMWF ocean reanalysis system ORAS4. *Quarterly Journal of the Royal Meteorological Society*, 139, 1132–1161.
- Bauer, P., Thorpe, A., & Brunet, G. (2015). The quiet revolution of numerical weather prediction. *Nature*, 525(7567), 47–55.
- Gadgil, S., & Gadgil, S. (2006). The Indian monsoon, GDP and agriculture. *Economic and Political Weekly*, 4887–4895.
- Huang, B., Banzon, V. F., Freeman, E., Lawrimore, J., Liu, W., Peterson, T. C., et al. (2014). Extended reconstructed sea surface temperature version 4 (ERSST.v4): Part I. Upgrades and intercomparisons. *Journal of Climate*, 28, 911–930. <https://doi.org/10.1175/JCLI-D-14-0006.1>
- Huang, B., Shin, C. S., Shukla, J., Marx, L., Balmaseda, M., Halder, S., et al. (2017). Reforecasting the ENSO events in the past fifty-seven years (1958–2014). *Journal of Climate*. <https://doi.org/10.1175/JCLI-D-16-0642.1>
- Huang, B., Zhu, J., Marx, L., Wu, X., Kumar, A., Hu, Z. Z., et al. (2015). Climate drift of AMOC, North Atlantic salinity and arctic sea ice in CFSv2 decadal predictions. *Climate Dynamics*, 44, 559–583. <https://doi.org/10.1007/s00382-014-2395-y>
- Joshi, U. R., & Rajeevan, M. (2006). Trends in precipitation extremes over India. National Climate Centre. India Meteorological Department. Research Report No: 3/2006.
- Kim, H.-M., Webster, P. J., Curry, J. A., & Toma, V. (2012). Asian summer monsoon prediction in ECMWF system 4 and NCEP CFSv2 retrospective seasonal forecasts. *Climate Dynamics*, 39, 2975–2991.
- Kirtman, B. P., & Shukla, J. (2000). Influence of the Indian summer monsoon on ENSO. *Quarterly Journal of the Royal Meteorological Society*, 126, 213–239.
- Krishna Kumar, K., Rajagopalan, K. B., & Cane, M. A. (1999). On the weakening relationship between the Indian monsoon and ENSO. *Science*, 284, 2156–2159.
- Kulkarni, M. A., Acharya, N., Kar, S. C., Mohanty, U. C., Tippett, M. K., Robertson, A. W., et al. (2012). Probabilistic prediction of Indian summer monsoon rainfall using global climate models. *Theoretical and Applied Climatology*, 107, 441–450.
- Lau, N. C., & Nath, M. J. (2000). Impact of ENSO on the variability of the Asian-Australian monsoons as simulated in GCM experiments. *Journal of Climate*, 13, 4287–4307.
- Levine, R. C., Turner, A. G., Marathayil, D., & Martin, G. M. (2013). The role of northern Arabian Sea surface temperature biases in CMIP5 model simulations and future projections of Indian summer monsoon rainfall. *Climate Dynamics*, 41, 155–172. <https://doi.org/10.1007/s00382-012-1656-x>
- Liu, W., Huang, B., Thorne, P. W., Banzon, V. F., Zhang, H.-M., Freeman, E., et al. (2014). Extended reconstructed sea surface temperature version 4 (ERSST.v4): Part II. Parametric and structural uncertainty estimations. *Journal of Climate*, 28, 931–951. <https://doi.org/10.1175/JCLI-D-14-00007.1>
- Pai, D. S., Sridhar, L., Rajeevan, M., Sreejith, O. P., Satbhai, N. S., & Mukhopadyay, B. (2013). Development and analysis of a new high spatial resolution ( $0.25 \times 0.25$ ) long period (1901–2010) daily gridded rainfall dataset over India. NCC Reserach Report No. 1/2013, National Climate Centre, India Meteorological Department, Pune, India, pp 70.
- Palmer, T. N., Doblas-Reyes, F. J., Hagedorn, R., & Weisheimer, A. (2005). Probabilistic prediction of climate using multi-model ensembles: From basics to applications. *Philosophical Transactions of the Royal Society of London. Series B, Biological Sciences*, 360(1463), 1991–1998. <https://doi.org/10.1098/rstb.2005.1750>
- Rasmusson, E. M., & Carpenter, T. H. (1983). The relationship between eastern equatorial Pacific sea surface temperature and rainfall over India and Sri Lanka. *Monthly Weather Review*, 111, 517–528.
- Reynolds, R. W., & Smith, T. M. (1995). A high-resolution global sea surface temperature climatology. *Journal of Climate*, 7, 1571–1583.
- Rodell, M., Houser, P. R., Jambor, U., Gottschalck, J., Mitchell, K., Meng, C.-J., et al. (2004). The global land data assimilation system. *Bulletin of the American Meteorological Society*, 85(3), 381–394.
- Rui, H., & Beaudoing, H. (2015). README document for Global Land Data AssimilationSystem version 2 (GLDAS-2) products. NASA Goddard Earth Sciences Data and Information Services Center Tech. Doc., 23 pp.
- Saha, S., Moorthi, S., Pan, H.-L., Wu, X., Wang, J., Nadiga, S., et al. (2010). The NCEP Climate Forecast System Reanalysis. *Bulletin of the American Meteorological Society*, 91(8), 1015–1057. <https://doi.org/10.1175/2010BAMS3001.1>
- Saha, S., Moorthi, S., Wu, X., Wang, J., Nadiga, S., Patrick, T., et al. (2014). The NCEP climate forecast system version 2. *Journal of Climate*, 27, 2185–2208.
- Saha, S. K., Hazra, A., Pokhrel, S., Chaudhari, H. S., Sujith, K., Rai, A., et al. (2019). Unraveling the mystery of Indian summer monsoon prediction: Improved estimate of predictability limit. *Journal of Geophysical Research: Atmospheres*, 124, 1962–1974. <https://doi.org/10.1029/2018JD030082>
- Sahana, A. S., & Ghosh, S. (2018). An improved prediction of Indian summer monsoon onset from state of the art dynamic model using physics guided data driven approach. *Geophysical Research Letters*, 45(16), 8510–8518. <https://doi.org/10.1029/2018GL078319>
- Shin, C. S., Huang, B., Zhu, J., Marx, L., & Kinter, J. L. (2019). Improved seasonal predictive skill and enhanced predictability of the Asian summer monsoon rainfall following ENSO events in NCEP CFSv2 hindcasts. *Climate Dynamics*. <https://doi.org/10.1007/s00382-018-4316-y>
- Shukla, J., & Paolin, D. A. (1983). The southern oscillation and long range 698 forecasting of the summer monsoon rainfall over India. *Monthly Weather Review*, 111, 1830–1837.
- Shukla, R. P., & Huang, B. (2015). Mean state and interannual variability of the Indian summer monsoon simulation by NCEP CFSv2. *Climate Dynamics*. <https://doi.org/10.1007/s00382-015-2808-6>
- Shukla, R. P., Huang, B., Dirmeyer, P. A., & Kinter, J. L. (2019). The influence of summer deep soil temperature on early winter snow conditions in Eurasia in the NCEP CFSv2 simulation. *Journal of Geophysical Research: Atmospheres*, 124, 9062–9077. <https://doi.org/10.1029/2019JD030279>
- Shukla, R. P., Huang, B., Dirmeyer, P. A., Kinter, J. L., Shin, C.-S., & Marx, L. (2019). Climatological influence of Eurasian winter surface condition on the Asian and Indo-Pacific summer circulation in the CFSv2 seasonal reforecasts. *International Journal of Climatology*. <https://doi.org/10.1002/joc.6029>
- Shukla, R. P., Huang, B., Marx, L., Kinter, J. L., & Shin, C.-S. (2017). Predictability and prediction of Indian summer monsoon by CFSv2: Implication of the initial shock effect. *Climate Dynamics*. <https://doi.org/10.1007/s00382-017-3594-0>
- Towns, J., Cockerill, T., Dahan, M., Foster, I., Gaither, K., Grimshaw, A., et al. (2014). XSEDE: Accelerating scientific discovery. *Computing in Science & Engineering*, 16(5), 62–74. <https://doi.org/10.1109/MCSE.2014.80>
- Uppala, S. M., Källberg, P. W., Simmons, A. J., Andrae, U., Bechtold, V. D. C., Fiorino, M., et al. (2005). The ERA-40 re-analysis. *Quarterly Journal of the Royal Meteorological Society*, 131(612), 2961–3012. <https://doi.org/10.1256/qj.04.176>
- Wang, B., Wu, R., & Fu, X. (2000). Pacific–East Asian teleconnection: How does ENSO affect East Asian climate? *Journal of Climate*, 13, 1517–1536.

- Webster, P. J., & Yang, S. (1992). Monsoon and ENSO: Selectively interactive systems. *Quarterly Journal of the Royal Meteorological Society*, 118, 877–926.
- Zhu, J., Huang, B., Marx, L., Kinter, J. L. III, Balmaseda, M. A., Zhang, R.-H., & Hu, Z.-Z. (2012). Ensemble ENSO hindcasts initialized from multiple ocean analyses. *Geophysical Research Letters*, 39, L09602. <https://doi.org/10.1029/2012GL051503>
- Zhu, J., & Shukla, J. (2013). The role of air-sea coupling in seasonal prediction of Asia-Pacific summer monsoon rainfall. *Journal of Climate*, 26, 5689–5697.